Moment Behavior of Laminated Beam-Column Joint with Glued-In Steel Rods Manufactured from Small-Diameter Larch Logs

Been Ha
Keita Ogawa
Mariko Yamasaki
Yasutoshi Sasaki

Abstract

To promote the structural use of small-diameter logs often harvested in Korea, the use of laminated members with square timber obtained from small-diameter logs as their elements is being considered. With the objective of improved strength, elements obtained from large-diameter logs were combined with elements obtained from small-diameter logs. In this study, the authors prepared beam-column joints using these laminated members and examined their moment resistance performance. To join a laminated beam and a laminated column, the authors used glued-in steel rods. The results of a mechanical test on the moment–deformation angle relationship showed that from the initial force to the failure point, the behavior was mostly linear. Moreover, the rotational stiffness was approximately 900 kNm/rad, the maximum moment was approximately 30 kNm, and the joint efficiency for deformation was approximately 0.8. It was revealed that a significant amount of the deformation in this specimen resulted from the bending deflection of the laminated column. The authors also estimated the rotational stiffness and maximum moment through linear analysis. The slip properties of the deformed bar, compression properties perpendicular to grain of the laminated column, and bending properties of the laminated column were taken into consideration. The estimated results were mostly consistent with the experimental results. As a method to easily understand the moment resistance performance of these joints, the present proposed estimation method should be effective.

In forestry operations, small-diameter logs are always produced. In Korea, a large number of small-diameter logs are produced, and an effective utilization of them becomes an immediate issue. To effectively use these small-diameter logs, examining their use as structural material is an important issue in the revitalization of the forestry and forestry industry. There have been many studies that evaluated the mechanical performance and physical properties for the effective use of small-diameter logs (Green et al. 2005, 2008; Ishiguri et al. 2006; Langum et al. 2009). In Korea, logs with a diameter at breast height (DBH) of 60 to 170 mm are classified as small-diameter logs. According to a report by the Korea Forest Service and Korea Forestry Promotion Institute (2013), the ratio of small-diameter logs to the total cutting volume exceeds 70 percent. Their use as structural material is desired, but since small-diameter logs contain a high ratio of juvenile wood, their strength is low, and they have a high potential for cracking and warping. However, if the juvenile wood is removed from the small-diameter logs, the yield of lumber decreases. Thus, at present, the utilization of small-diameter logs as structural materials is insufficient.

To promote the structural use of small-diameter logs, the authors developed a laminated member that uses these small-diameter logs. By laminating square timber and

The authors are, respectively, Graduate Student, Lab. of Timber Engineering, Dept. of Forest and Environ. Resources Sci., Graduate School of Bioagric. Sci., Nagoya Univ., Nagoya, Japan (ha.been@e.mbox.nagoya-u.ac.jp); Researcher, Engineered Wood and Joints Lab., Dept. of Wood Engineering, Forestry and Forest Products Research Inst., Tsukuba, Japan (ogawakeita@ffpri.affrc.go.jp); and Associate Professor and Professor, Lab. of Timber Engineering, Dept. of Forest and Environ. Resources Sci., Graduate School of Bioagric. Sci., Nagoya Univ., Nagoya, Japan (marikoy@agr.nagoya-u.ac.jp, ysasaki@nagoya-u.jp [corresponding author]). This paper was received for publication in February 2017. Article no. 17-00017.

Forest Prod. J. 68(3):295–302.
doi:10.13073/FPJ-D-17-00017

laminae from large-diameter logs onto square timber from small-diameter logs, the authors attempted to secure their strength as a structural material. The bending performance of these laminated members as beam material and compression performance as column material were experimentally examined. The results showed strength performance that indicates their potential as structural material. Therefore, to actualize the structural use of these laminated members, in addition to the previously mentioned performances, the mechanical performance when joined must be understood.

A joint with glued-in steel rods is one of the appropriate joining methods of laminated beams and columns. By this method, a hole is drilled in a member, and a steel rod is placed in this hole. By filling the gap between the steel rod and the drill hole with adhesive, members are joined (Madsen 2000). Since this joining method hides the steel rod in the wood member, it has a superior appearance. Because it is unlikely to lead to the corrosion of the steel rod and can be achieved at low cost, its use in structures is being promoted. In addition, the mechanical performance of beam-column joints with glued-in steel rods was experimentally examined by Buchanan and Fairweather (1993), Inoue et al. (1997), and Buchanan et al. (2001). Currently, structures are being built using this joining method in many places around the world, including Europe. Serrano (2001) and Steiger et al. (2006) experimentally examined the slip performance of a steel rod. Based on their results, Yang et al. (2016) attempted a theoretical analysis of the moment–deformation angle relationship of the beam-column joints.

The authors are studying the mechanical performance of the structural use of laminated columns and beams with elements of small-diameter logs. In this study, the authors examine the moment resistance performance of joints that use glued-in steel rods with a laminated member as structural parts. In addition, the authors attempt a theoretical analysis of the rotational stiffness and maximum moment of the joint through a mechanical analysis.

Materials and Methods

Joint specimen

The authors prepared a full-size joint specimen consisting of a laminated beam and column. For the laminated column, the authors used small-diameter Korean larch (*Larix kaempferi* Carr.) logs. These small-diameter logs were approximately 20 years old and had a DBH of 120 to 139 mm. By providing timber sawing, drying, and finishing to this joint specimen, the authors ultimately prepared a piece of square timber with a cross-sectional area of 90 by 90 mm. As shown in Figure 1a, the cross-sectional structure of the laminated column was designed by gluing and laminating four square timber pieces ($W = 180$ mm and $D = 180$ mm). The length of the laminated column was more than 2,000 mm.

The laminated beam was also prepared with the same small-diameter larch log, as above. However, the ultimate cross-sectional area of square timber was 80 by 80 mm, and four pieces of square timber were glued and laminated together, as shown in Figure 1b. Furthermore, three layers of lamina with a thickness of 26.66 mm that were prepared with large-diameter Korean larch logs were laminated to the top and bottom (a total of six) to create a cross-sectional surface ($B = 160$ mm and $H = 320$ mm). These laminae were mechanical grade E14 (Young's modulus of 14 to 16 GPa) based on KS F 3021(Korean Standards Association 2010). The length of the laminated beam was 1,500 mm.

When preparing the laminated beam and column, the authors used the same adhesive as in the previous study (Ha et al. 2018). For the adhesion between the square timbers within the same layer (i.e., edge gluing), an aqueous polymer isocyanate (Shikajirusi PI BOND TP-111; Oshika Co. Ltd, Tokyo, Japan) was used. For the adhesion between layers (i.e., laminate adhesion), phenol resorcinol formaldehyde (Deernol D-40; Oshika Co. Ltd, Tokyo, Japan) was used.

For the joint with glued-in steel rods, the authors used a deformed bar with a diameter of 19 mm. This deformed bar was made of grade SD 400 (yield strength $\geq$ 400 MPa and tensile strength $\geq$ 560 MPa) based on KS D 3504 (Korean Standards Association 2011). As shown in Figure 1c, the authors first drilled a hole with a diameter of 24 mm from the laminated column side and inserted the deformed bar so that it embedded the laminated beam. The authors inserted four deformed bars (two rows and two columns). The deformed bars on the upper row were placed 280 mm from the bottom surface of the laminated beam ($g = 280$ mm), and the deformed bars on the bottom rows were inserted at 50 mm from the bottom surface of the laminated beam ($h = 50$ mm). The embedment length into the laminated beam was 400 mm or 450 mm ($l = 400$ and 450 mm). After inserting the deformed bar, the authors opened injection holes with a diameter of 8 mm in the laminated column and the laminated beam toward the deformed bar and filled the holes with an adhesive. For the adhesive, the authors used epoxy resins: E1 (YD-115; Kukdo Chemical Co. Ltd, Seoul, South Korea) and E2 (CB10T; Rotafix Ltd, London, UK).

By combining the embedment lengths in the laminated beam with these types of adhesive, the authors created four series of joint specimens: E1-400, embedment length of 400 mm into the laminated beam and E1 adhesive; E1-450, embedment length of 450 mm and E1 adhesive; E2-400, embedment length of 400 mm and E2 adhesive; and E2-450, embedment length of 450 mm and E2 adhesive.

Mechanical test for the joint specimen

A mechanical test of the joint was implemented, as shown in Figure 2. The laminated column and the laminated beam were fixed with the steel frame of the test mechanic (capacity 40 tons, DA-W260; Dongah Testing Machine Co., Seoul, South Korea) through a pin connection, as shown in the figure. By applying lateral load P from the actuator connected to the laminated beam through a steel beam, a moment M was applied to the joint. As shown in the figure, by attaching a load cell, P was measured. In addition, as shown in the figure, by attaching linear variable differential transformer (LVDT) (DEX-01-V; Mutoh Engineering Inc., Tokyo, Japan), the authors measured the lateral displacement δ in the laminated beam. M and deformation angle θ of the joint were calculated using the read value of load cell P, read value of LVDT δ, and length of the moment arm L ($L =$ 2,000 mm):

$$M = PL \tag{1}$$

$$\theta \approx \tan\theta = \frac{\delta}{L} \tag{2}$$

The load was applied with displacement control, and a reverse cyclic load was used. The authors set 10 cyclic steps

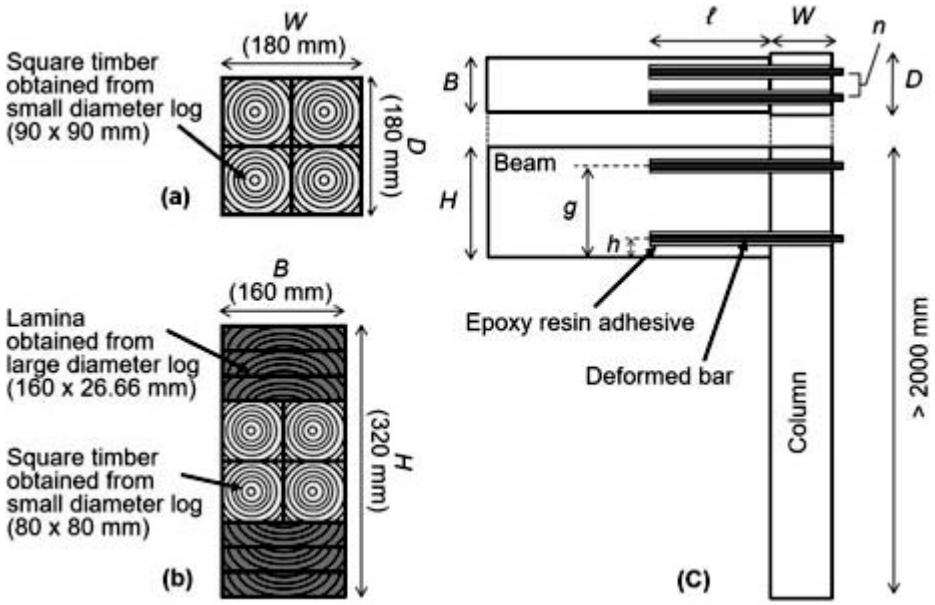

Figure 1.—Beam-column joint with glued-in steel rods: (a) cross-sectional structure of laminated column, (b) cross-sectional structure of laminated beam, and (c) joint specimen.

for the turning point of the load with deformation angles of ±1/2,000, 1/666, 1/400, 1/285, 1/200, 1/133, 1/100, 1/66, 1/50, and 1/40 rad and repeated three identical cycles at each step. Subsequently, the load was applied monotonously until the joint failed. The load rate was set at 100 mm/min.

In the photo in Figure 2, there is an additional short lateral member around the joint part. It was attached for another purpose. Because this research discusses only the moment resistance behavior of the laminated beam and column joint, the existence of the attached member could be ignored.

Pull-in test for glued-in steel rods

When a mechanical test of the joint is implemented, as shown in Figure 2, a pull-in load or a pull-out load is applied to glued-in steel rods. Before the theoretical analysis for the moment resistance of the joint, the pull-in test for the deformed bar embedded in the member was conducted, as shown in Figure 3. It is supposed that pull-in load and pull-out load are the same. As shown in the figure, the authors prepared a specimen laminated from larch laminae with a height of 200 mm using a deformed bar with a diameter of 19 mm and two types of epoxy resin adhesives, as in the earlier joint specimen. The authors applied the load from the top of the deformed bar downward. At this time, based on the relationship between the load and the slip displacement, the authors obtained the maximum load and slip modulus in a pull-in test, as shown in Table 1.

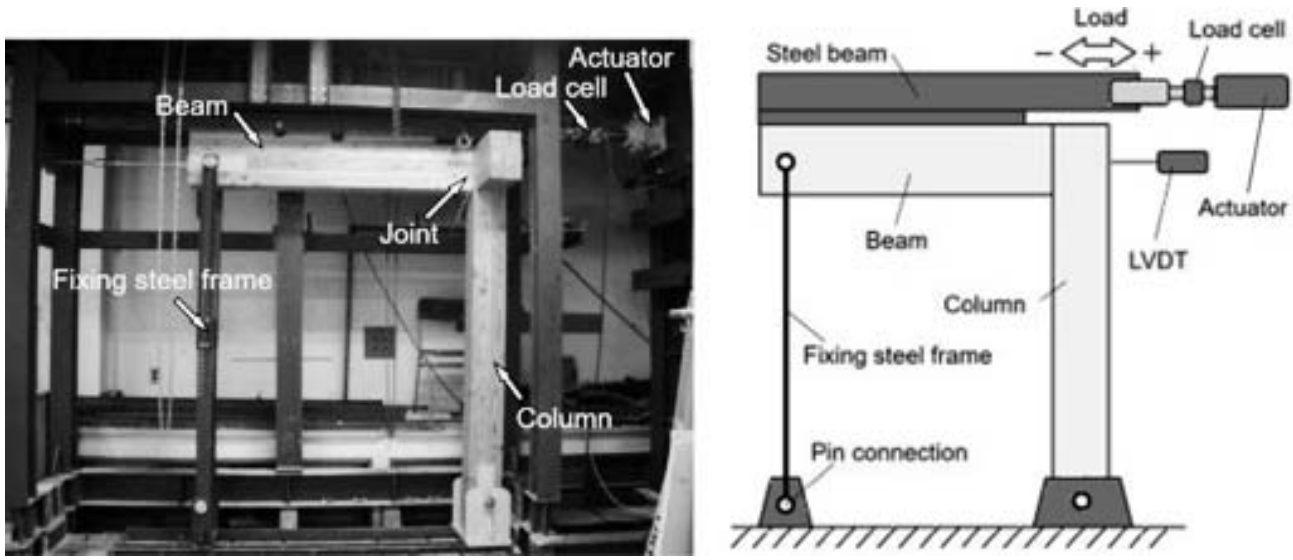

Figure 2.—Mechanical test method for joint specimen.

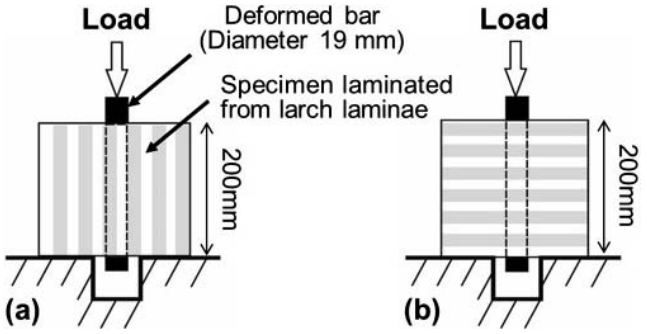

Figure 3.—Pull-in test method for glued-in steel rods: (a) parallel to grain and (b) perpendicular to grain.

Experimental Results

Moment–deformation angle relationship and failure mode

Figure 4 shows the moment–deformation angle relationship obtained from the mechanical test. The figure shows a typical example from each series. According to the figure, for all series, from the initial force to the failure point, the behavior was highly linear. In addition, the energy loss was small. When it reached the failure point, the moment value rapidly decreased. In other words, brittle failure was exhibited. The failure at this time is shown in Figure 5. The bending failure of the laminated column occurred around the joint before the moment reached the joint capacity. It means that the joint design of the joint specimen was overdesigned.

In the joint specimen used in this study, the cross section of the laminated column was not sufficiently large relative to the moment resistance performance of the joint. Therefore, for the deformation of the specimen, the ratio of the bending deformation of the laminated column was high. Therefore, in a moment–deformation angle relationship, as shown in Figure 4, the bending behavior of the laminated column was strongly reflected. As a result, brittle behavior was exhibited by the joint specimen.

Mechanical properties from the moment–deformation angle relationship

The authors calculated and obtained the following mechanical properties from the moment–deformation angle relationship: rotational stiffness K, maximum moment $M_{\max}$, deformation angle at the maximum moment $\theta_{\max}$, moment at the deformation angle 1/120 rad $M_{1/120}$, strain energy U, and joint efficiency for deformation $\delta_{C,\max}/\delta_{\max}$. K was obtained by regressing the linear portion of the moment–deformation angle relationship and taking the slope. U was obtained as the area surrounded by the moment–deformation angle curve from the initial force to the failure point. In addition, $\delta_{C,\max}/\delta_{\max}$ was obtained by dividing the bending deflection in the upper portion of the laminated column at the maximum lateral load in the load cell values $\delta_{C,\max}$ (obtained from Equation 13 below) by the lateral displacement at the maximum lateral load in the LVDT values $\delta_{\max}$.

Table 1.—Pull-in test results for glued-in steel rods at embedment length of 200 mm in member.

Adhesive	Embedment direction	Maximum load (kN)	Slip modulus (kN/mm)
E1	Parallel to grain	72.9	101.8
E1	Perpendicular to grain	127.4	74.5
E2	Parallel to grain	105.7	76.3
E2	Perpendicular to grain	124.0	67.5

Table 2 gives the results of the experimentally obtained properties. K of the series E1-400 and series E1-450 are 965.6 and 916.3 kNm/rad (mean value), respectively, which were slightly higher than K of the series E2-400 and series E2-450 (mean 879.2 and 902.6 kNm/rad, respectively). In addition, $M_{\max}$ and $M_{1/120}$ were also slightly higher for the series E1-400 and series E1-450 compared to the series E2-400 and E2-450. Because the mean values seemed to be decided not only by adhesive performance but also by column strength, it is difficult for selecting the most suitable adhesive for the joint. Further discussion is needed for the selection of adhesion. On the other hand, if the authors focus on the difference in embedment length of the deformed bar into the laminated beam, it was expected that the performance would improve with the embedment length. However, in the present experiment, this effect could not be clearly confirmed; $\delta_{C,\max}/\delta_{\max}$ showed a high value (mean 0.78 to 0.93) for all four series. Therefore, in the present mechanical test, it was confirmed that the majority of the joint specimen deformation was the bending deformation of the laminated column because the rotational deformation of the joint part had an adequate performance.

Theoretical Analysis

Rotational stiffness of the joint part

By modeling the mechanism of proof stress expression, the authors estimated the rotational stiffness K and maximum moment $M_{\max}$ of this joint specimen. As shown in Figure 2, when lateral load P is applied to the joint and moment M is acting on it, the following events occur: (1) slip between the deformed bar and member and (2) deformation due to compression perpendicular to grain by the laminated beam on the laminated column. In addition, the authors considered (3) bending deformation of the laminated column by P.

The authors expressed the rigidity of the laminated column against the compression perpendicular to grain and slip modulus in a pull-in test of the deformed bar at the joint. This test used the spring model shown in Figure 6. The figure shows a rotational deformation of the joint, where k_{s0} and k_{s90} are the slip modulus in the pull-in test when the deformed bar was inserted parallel to grain and perpendicular to grain, respectively, while k_{pc} is the rigidity for compression perpendicular to grain of the laminated column. To obtain the values of k_{s0} and k_{s90}, the authors implemented the pull-in test, as shown in Figure 3.

The neutral axis of the joint was assumed to be at a distance of λ from the bottom of the laminated beam. The area above the axis was considered to be under compression, while the area below the axis was considered to be under tension. As the springs of k_{s0} and k_{s90} are connected in series, the slip rigidity for the deformed bar on the tension side k_T is

$$k_T = \frac{k_{s0} \cdot k_{s90}}{k_{s0} + k_{s90}} \times n \tag{3}$$

where n is number of columns for deformed bars ($n = 2$ for the present specimen). When the deformation angle of

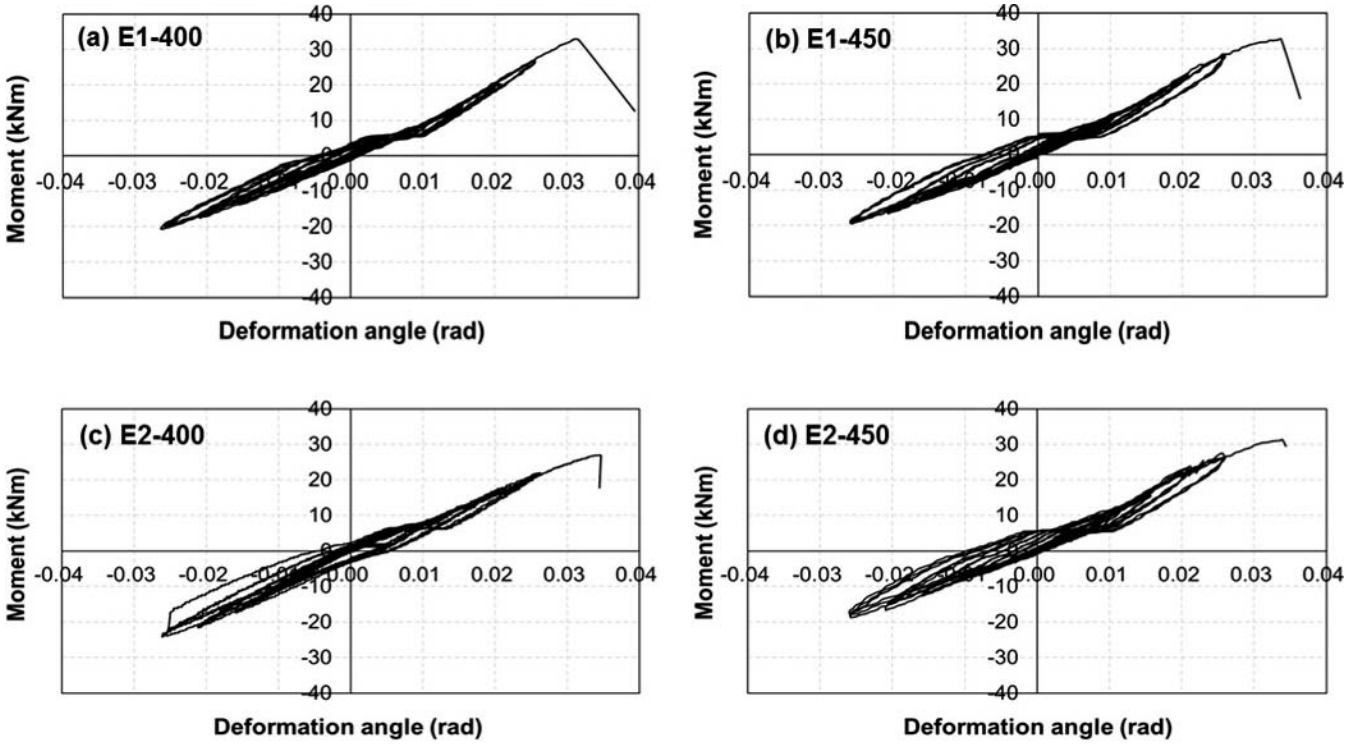

Figure 4.—Moment–deformation angle relationship obtained from mechanical test.

rotational deformation at the joint is θ_J, the amount of slip for the deformed bar on the tension side is $(\lambda - h)\ \theta_J$ and tensile force T is expressed as follows:

$$T = k_T(\lambda - h)\theta_J \tag{4}$$

On the other hand, the slip rigidity for the deformed bar on the compression side k_C is the same as in Equation 3:

$$k_C = \frac{k_{s0} \cdot k_{s90}}{k_{s0} + k_{s90}} \times n \tag{5}$$

On the compression side, there is a triangular compression deformation perpendicular to grain on the laminated column. Column compression resistance load P_{pc} is expressed using the rigidity for compression perpendicular to grain of the laminated column k_{pc}:

$$P_{pc} = k_{pc} \cdot \frac{H - \lambda}{2}\theta_J \tag{6}$$

The amount of slip for the deformed bar on the compression side is $(g - \lambda)\ \theta_J$, and compressive force C is expressed with the sum of the force on the deformed bar and P_{pc}:

$$C = k_C(g - \lambda)\theta_J + P_{pc} \tag{7}$$

From here, distance λ from the bottom of the laminated beam and the neutral axis is obtained. Based on the balance of lateral forces on the joint,

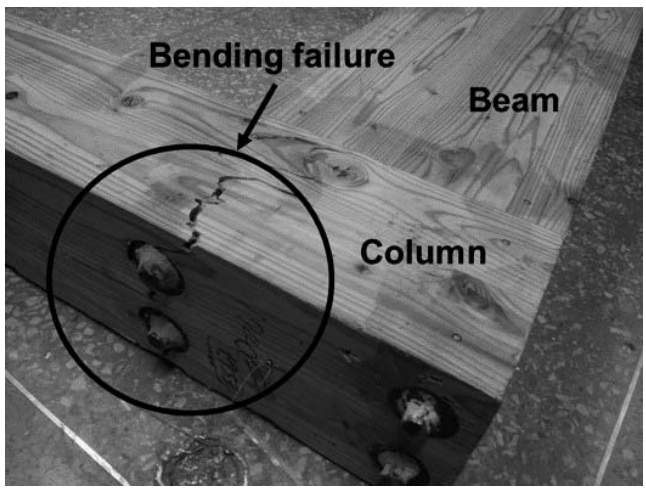

Figure 5.—Bending failure of laminated column.

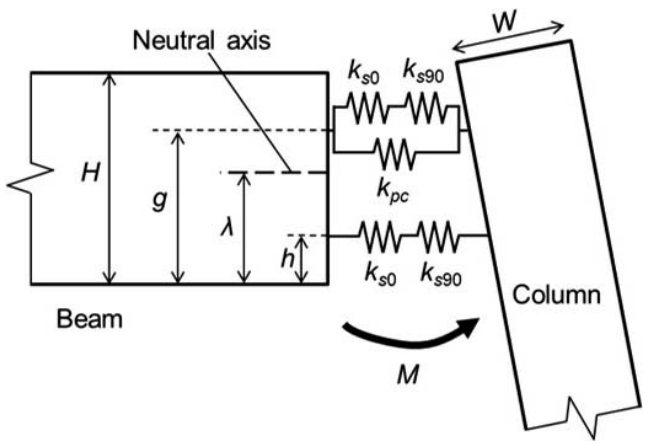

Figure 6.—Spring model of joint under joint rotational deformation at θ_J rad.

Table 2.—Mechanical properties of joint specimen.[a]

Series	Specimen no.	K (kNm/rad)	M_{max} (kNm)	θ_{max} (rad)	$M_{1/120}$ (kNm)	U (kNmrad)	$\delta_{C,max}/\delta_{max}$
E1-400	1	1020.3	35.9	0.032	8.3	0.57	0.94
	2	920.6	29.6	0.026	7.3	0.37	0.97
	3	956.1	32.9	0.031	6.4	0.49	0.90
	Average	965.6	32.8	0.030	7.3	0.47	0.93
E1-450	1	960.7	29.2	0.026	6.9	0.35	0.96
	2	954.1	32.6	0.034	8.1	0.60	0.82
	3	834.3	25.6	0.026	7.2	0.32	0.84
	Average	916.3	29.1	0.028	7.4	0.42	0.87
E2-400	1	915.9	27.7	0.028	7.1	0.39	0.82
	2	887.2	26.9	0.034	7.4	0.50	0.66
	3	834.4	25.4	0.023	6.2	0.33	0.93
	Average	879.2	26.7	0.029	6.9	0.41	0.80
E2-450	1	922.1	31.3	0.034	7.2	0.58	0.78
	2	881.6	24.1	0.026	6.0	0.30	0.80
	3	904.3	27.8	0.031	7.8	0.45	0.75
	Average	902.6	27.7	0.030	7.0	0.45	0.78

[a] K = rotational stiffness; M_{max} = maximum moment; θ_{max} = deformation angle at M_{max}; $M_{1/120}$ = moment at deformation angle 1/120 rad; U = strain energy; $\delta_{C,max}/\delta_{max}$ = joint efficiency for deformation.

$$T = C \tag{8}$$

and when Equations 4 and 7 are substituted, the following equation is obtained:

$$k_T(\lambda - h)\theta_J = k_C(g - \lambda)\theta_J + k_{pc} \cdot \frac{H - \lambda}{2}\theta_J \tag{9}$$

As Equation 9 is the quadratic equation of λ, λ can be obtained as follows:

$$\lambda = \frac{2k_T h + 2k_C g + k_{pc} H}{2k_T + 2k_C + k_{pc}} \tag{10}$$

M around the neutral axis is expressed as the sum of the moment of the deformed bar on the tension side, the moment of the deformed bar on the compression side, and the moment of resistance of the triangular compression perpendicular to grain on the laminated column:

$$M = k_T(\lambda - h)^2\theta_J + k_C(g - \lambda)^2\theta_J + k_{pc}\frac{H - \lambda}{2}\theta_J \cdot \frac{2}{3}(H - \lambda) \tag{11}$$

Rotational stiffness of the joint part K_J is expressed using the following equation:

$$K_J = \frac{M}{\theta_J} = k_T(\lambda - h)^2 + k_C(g - \lambda)^2 + k_{pc}\frac{(H - \lambda)^2}{3} \tag{12}$$

Bending deformation of the laminated column

Next, the bending deformation of the laminated column is considered. If the bending mode in the laminated column is assumed to be the same as that of a cantilever, the amount of bending deflection δ_C can be obtained with the following equation:

$$\delta_C = \frac{PL^3}{3EI} \tag{13}$$

where L, E, and I are the distance from the center of the joint part to pin connected part in the bottom of laminated column (equal to the length of moment arm mentioned above), bending Young's modulus, and the moment of inertia ($I = DW^3/12$), respectively. $M = PL$; thus, Equation 13 can be expressed as follows:

$$M = \frac{3EI}{L^2} \cdot \delta_C \tag{14}$$

δ_C is expressed as deformation angle θ_c in the present test. As $\theta_C = \delta_C/L$ is true, Equation 14 becomes

$$M = \frac{3EI}{L}\theta_C \tag{15}$$

Moment resistance performance of the joint specimen

Total deformation angle θ for the joint specimen is expressed as the sum of θ_J and θ_C. When Equations 12 and 15 are substituted,

$$\theta = \theta_J + \theta_C = M\left(\frac{1}{K_J} + \frac{L}{3EI}\right) \tag{16}$$

Therefore, the rotational stiffness of the joint specimen K can be obtained from the following equation:

$$K = \frac{M}{\theta} = \frac{K_J \cdot 3EI}{K_J L + 3EI} \tag{17}$$

In addition, the failure point of the joint specimen is determined by the bending failure of the laminated column, as shown in Figure 5. If the bending failure of the laminated column is equal to maximum moment M_{max}, it can be obtained using the bending strength of the laminated column σ_{max}:

$$M_{max} = \frac{\sigma_{max} DW^2}{6} \tag{18}$$

Theoretical estimation of the moment resistance performance

Rotational stiffness K and maximum moment M_{max} obtained in Equations 17 and 18 were compared with the

results of the experiment. The dimensional parameters for the joint specimen are as follows: $W = 180$ mm, $D = 180$ mm, $L = 2{,}000$ mm, $B = 160$ mm, $H = 320$ mm, $g = 280$ mm, and $h = 50$ mm. The embedment length of the deformed bar into the laminated beam l was as follows: $l = 400$ mm for the series E1-400 and series E2-400, and $l = 450$ mm for the series E1-450 and series E2-450. In addition, the number of columns for the deformed bar was set at $n = 2$.

As shown Table 1, the slip modulus in the pull-in test obtained from the additional test was 101.8 and 74.5 kN/mm parallel and perpendicular to grain, respectively, when adhesive E1 was used. When adhesive E2 was used, the slip modulus was 76.3 and 67.5 kN/mm for the parallel and perpendicular to grain, respectively. However, these were slip modulus in the pull-in test when the embedment length of the deformed bar was 200 mm. To apply this to a mechanical analysis of the joint, for slip modulus in the parallel to grain (laminated beam), the authors multiplied the above values for the parallel to grain by $l/200$: k_{s0}.

Similarly, for slip perpendicular to grain (laminated column), the above values for the perpendicular to grain were multiplied by $W/200$: k_{s90}. Regarding rigidity for compression perpendicular to grain of the laminated column k_{pc}, it is desired to conduct an additional test with wood species that have the same size and loading mode. However, the authors could not conduct the test. Thus, the rigidity k_{pc} was calculated with modulus of elasticity in radial direction compression E_{90} with the following equation:

$$k_{pc} = E_{90}\frac{B(H-\lambda)}{w} \tag{19}$$

Then the value of $E_{90} = 1.70$ GPa was used (Iijima 1983). For the bending Young's modulus E and bending strength $\sigma_{\max}$ of the laminated column, the authors used test results for a laminated member similar to the one tested in a previous study: $E = 9.0$ GPa and $\sigma_{\max} = 27.6$ MPa (Ha et al. 2018).

In this research, theoretical analysis was assumed by the linearly elastic response of the laminated column in compression perpendicular to grain. To check the validity of this assumption, the authors compared calculated compressive stress σ_{cal90} for perpendicular to grain at the maximum moment with the stress at proportional limit σ_{90} for compression perpendicular to grain of the laminated column. The compressive stress σ_{cal90} is expressed using the following equation by dividing P_{pc} by the loaded area:

$$\sigma_{cal90} = \frac{P_{pc}}{B(H-\lambda)} = E_{90}\frac{(H-\lambda)}{2W}\theta_J \tag{20}$$

where the column compression resistance load P_{pc} was obtained from Equation 6 and the deformation angle of rotational deformation at the joint θ_J was obtained from Equation 12 at the maximum moment. The value of σ_{cal90} was varied with specimen series and was in the range of 3.6 to 4.0 MPa. According to the Ido et al. (2010), σ_{90} was 3.3 MPa on average with a standard deviation of 1.1 MPa. Comparing the values, the possibility that the compression of the laminated column was in the elastic region during the mechanical test was revealed. Although the yielding might be occurred at the large deformation angle, the authors considered that it was not a significant issue because of the estimated result shown later.

Figure 7 shows a comparison between the experimental (thin solid line) and estimated (thick solid line) results. The estimated results for both K and $M_{\max}$ are consistent with the test results. The results for all specimen series are summarized in Table 3. According to these results, estimated results were slightly lower than the test results (safety side), but this was considered to be consistent. Therefore, the authors were able to confirm the validity of the proposed estimation method; that is, the moment resistance performance of the present joint specimen can be expressed using the slip properties of the deformed bar, compression properties perpendicular to grain of the laminated column, and bending properties of the laminated column. The present laminated beam is a mixture of elements derived from both small- and large-diameter logs, but the moment resistance performance of the joint can be expressed by a simple model, as shown in Figure 6.

In Figure 7, the dashed line represents the estimated result if the rotational stiffness of the joint part K_J (obtained from Equation 12) is taken as infinite, except the bending deformation of the laminated column. Table 3 shows K_J and the stiffness by the column bending deformation K_C ($K_C = M/\theta_C$). K_J values ranged from 3,315.8 to 3,834.2 kNm/rad, which is much higher than the estimated K values (870.8 to 902.9 kNm/rad), while K_C was 1,181.0 kNm/rad. This was similar to the result of the joint efficiency for deformation $\delta_{C,\max}/\delta_{\max}$ obtained from the mechanical test of the joint specimen, and it was shown that the bending deformation of the laminated column was included in the joint specimen deformation.

In a previous study (Ha et al. 2018), the laminated members reinforced with large-diameter logs had higher bending strength and Young's modulus than the laminated members using only small-diameter logs, and the bending Young's modulus of these reinforced laminated members had values either the same as or higher than the general glulam. If the reinforcement method were attempted on the laminated column, the bending deformation might become smaller and the rotational stiffness of the joint specimen might approach K_J.

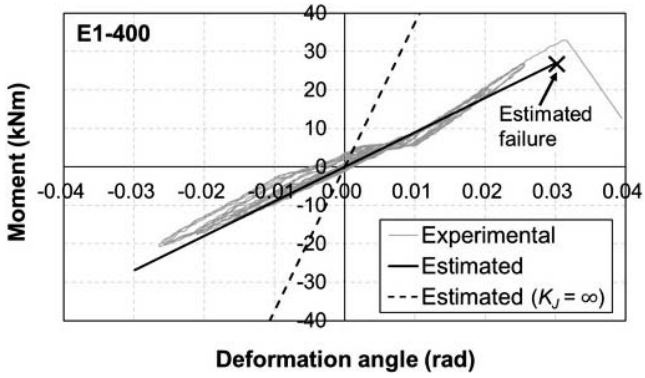

Figure 7.—Comparison of experimental and estimated results for moment–deformation angle relationship.

Table 3.—Comparison of experimental and estimated results for mechanical properties.[a]

Series	Experimental			Estimated				
	K (kNm/rad)	M_{max} (kNm)	θ_{max} (rad)	K_J (kNm/rad)	K_C (kNm/rad)	K (kNm/rad)	M_{max} (kNm)	θ_{max} (rad)
E1-400	965.6	32.8	0.030	3747.2	1181.0	898.0	26.8	0.030
E1-450	916.3	29.1	0.028	3834.2	1181.0	902.9	26.8	0.030
E2-400	879.2	26.7	0.029	3315.8	1181.0	870.8	26.8	0.031
E2-450	902.6	27.7	0.030	3404.3	1181.0	876.8	26.8	0.031

[a] K = rotational stiffness; M_{max} = maximum moment; θ_{max} = deformation angle at M_{max}; K_J = rotational stiffness of joint part; K_C = stiffness by the column bending deformation.

Conclusions

To promote the structural use of small-diameter logs, the authors prepared a beam-column joint using a laminated member with square timber obtained from small-diameter logs as elements and examined its moment resistance performance. To join a laminated beam and laminated column, the authors applied glued-in steel rods. The results of a mechanical test that examined the moment–deformation angle relationship showed mostly linear behavior from initial force to failure point. In addition, the rotational stiffness ranged between 879.2 and 965.6 kNm/rad (mean value for each series), and the maximum moment ranged between 26.7 and 32.8 kNm (mean value for each series). Although there was a difference in performance based on the type of adhesive, there was no difference in performance based on the embedment length of the deformed bar. In addition, joint efficiency for deformation ranged between 0.78 and 0.93 (mean value for each series), and deformation of the present specimen was dominated by the bending deflection of the laminated column. Based on the observation of failure, the failure of the present specimen was determined by the bending failure of the laminated column.

Based on these results, the authors performed a linear analysis based on a theoretical discussion. The authors obtained a rotational deformation of the joint from slip properties of the deformed bar and compression properties perpendicular to grain of the laminated column. In addition, by considering the bending deformation of the laminated column from the bending properties of the laminated column, the rotational stiffness and maximum moment of the joint specimen were estimated. The estimated results were consistent with the experimental results. The rotational stiffness of the joint part estimated in this process ranged between 3315.8 and 3834.2 kNm/rad. By reinforcing the bending performance of the laminated column, it was suggested that the rotational stiffness of the joint specimen could approach the estimated value.

As can be seen from the above results, the authors were able to confirm the possibility as the structural design of the laminated beam–column joint with glued-in steel rods using small-diameter logs. The test and theoretical result revealed two points: most of the deformation of the specimen was occupied by the column bending, and the joint part had enough rotational performance for structural usage. In terms of the column bending, it does not seem to be a significant issue because the authors had already reported the reinforcement method (Ha et al. 2018). These discussion results can contribute to the promotion of the structural use of small-diameter logs.

Acknowledgments

This research was financially supported from the Korea Forest Service (Project No. S121214L090110), Daejeon, South Korea.

Literature Cited

Buchanan, A. H. and R. H. Fairweather. 1993. Seismic design of glulam structures. *Bull. New Zeal. Natl. Soc. Earthquake Eng*. 26(4):415–436.

Buchanan, A., P. Moss, and N. Wong. 2001. Ductile moment-resisting connections in glulam beams. *In:* Proceedings of the New Zealand Society for Earthquake Engineering Conference, March 23–25, 2001, Wairakei, Taupo; New Zealand Society for Earthquake Engineering Inc., Wellington. Paper No. 6.02.01.

Green, D. W., T. M. Gorman, J. W. Evans, J. F. Murphy, and C. A. Hatfield. 2008. Grading and properties of small-diameter Douglas-fir and ponderosa pine tapered logs. *Forest Prod. J*. 58(11):33–41.

Green, D. W., E. C. Lowell, and R. Hernandez. 2005. Structural lumber from dense stands of small-diameter Douglas-fir trees. *Forest Prod. J*. 55(7/8):42–50.

Ha, B., S. S. Jang, K. Ogawa, M. Yamasaki, and Y. Sasaki. 2018. Strength and rigidity performance of laminated members using small-diameter logs. *Forest Prod. J*. 68(1):54–63.

Ido, H., H. Nagao, H. Kato, A. Miyatake, and Y. Hiramatsu. 2010. Strength properties of laminated veneer lumber in compression perpendicular to its grain. *J. Wood Sci*. 56:422–428.

Iijima, Y. 1983. The mechanical properties of the Siberian larch wood. *Bull. Toyama Wood Prod. Res. Inst*. 1:1–40. (In Japanese.)

Inoue, M., Y. Goto, Y. Goto, and Y. Eto. 1997. Experimental study on strength of connections composed of metal connecter and adhesive in timber structures. *J. Struct. Constr. Eng*. 498:105–111. (In Japanese.)

Ishiguri, F., J. Eisawa, Y. Saito, K. Iizuka, S. Yokota, and N. Yoshizawa. 2006. Comparison of wood properties of hinoki (*Chamaecyparis obsta*) small diameter logs collected from different tree ages and heights. *Mokuzai Gakkaishi* 52(6):383–388. (In Japanese.)

Korea Forest Service and Korea Forestry Promotion Institute. 2013. Assessment of the Korea's Forest Resources. Korea Forestry Promotion Institute, Seoul. pp. 94, 254. (In Korean.)

Korean Standards Association. 2010. Structural glued laminated timber. KS F 3021. Korean Standards Association, Seoul. (In Korean.)

Korean Standards Association. 2011. Steel bars for concrete reinforcement. KS D 3504. Korean Standards Association, Seoul. (In Korean.)

Langum, C. E., V. Yadama, and E. C. Lowell. 2009. Physical and mechanical properties of young-growth Douglas-fir and western hemlock from western Washington. *Forest Prod. J*. 59(11/12):37–47.

Madsen, B. 2000. Behavior of Timber Connections. Timber Engineering Ltd, North Vancouver, British Columbia, Canada. pp. 215–288.

Serrano, E. 2001. Glued-in rods for timber structures—An experimental study of softening behavior. *Mater. Struct*. 34:228–234.

Steiger, R., E. Gehri, and R. Widmann. 2006. Pull-out strength of axially loaded steel rods bonded in glulam parallel to the grain. *Mater. Struct*. 40:69–78.

Yang, H., W. Liu, and X. Ren. 2016. A component method for moment-resistant glulam beam-column connections with glued-in steel rods. *Eng. Struct*. 115:42–54.